Preliminary In-Flight Boundary Layer Transition Measurements on a 45-Degree Swept Wing at Mach Numbers Between 0.9 and 1.8

J. Blair Johnson

March 1988

NASA

National Aeronautics and
Space Administration

Preliminary In-Flight Boundary Layer Transition Measurements on a 45-Degree Swept Wing at Mach Numbers Between 0.9 and 1.8

J. Blair Johnson
Ames Research Center, Dryden Flight Research Facility, Edwards, California

1988

CONTENTS

SUMMARY

A preliminary flight experiment was flown to generate a full-scale supersonic data base to aid the assessment of computational codes, to improve instrumentation for measuring boundary layer transition at supersonic speeds, and to provide preliminary information for the definition of follow-on programs. The experiment was conducted using an F-15 aircraft that was modified with a small cleanup test section on the right wing. Results are presented for Mach (M) numbers from 0.9 to 1.8 at altitudes from 26,000 to 55,000 ft. They were combined to give a unit Reynolds number range of 1.7 to 4.0 million per ft. Angle of attack varied from approximately -1° to 10°.

At M ⩾ 1.2, transition occurred near or at the leading edge for the clean configuration. The furthest aft that transition was measured was 20 percent chord at M = 0.9 and M = 0.97. No change in transition location was observed after the addition of a notch-bump on the leading edge of the inboard side of the test section which was intended to minimize attachment line transition problems.

Some flow visualization was attempted during the flight experiment with both subliming chemicals and liquid crystals. However, difficulties arose from the limited time the test aircraft was able to hold test conditions and the difficulty of positioning the photo chase aircraft during supersonic test points. Therefore, no supersonic transition results were obtained using flow visualization.

INTRODUCTION

Recently, there has been a renewed interest in the feasibility of obtaining significant amounts of laminar flow at supersonic speeds. Although some supersonic boundary layer transition work was done on wings in the late 1950s (Banner and others, 1958; McTigue and others, 1959) and on the Arnold Engineering Development Center 10°-transition cone (Fisher and Dougherty, 1982), the most recent and extensive boundary layer transition work on lifting surfaces has concentrated on the transonic speed region (Runyan and others, 1984; Meyer and others, 1987). In addition, the development and increased sophistication of computational codes have led to a need for a large full-scale experimental data base to validate these codes.

Consequently, the NASA Ames-Dryden Flight Research Facility at Edwards, California conducted a preliminary flight experiment during the winter and spring of 1986 using an F-15 aircraft. The objectives of the flight experiment were to generate a full-scale supersonic data base for assessing computational tools, to improve instrumentation for measuring boundary layer transition at supersonic speeds, and to provide information for the definition of follow-on programs.

The flight experiment examined Mach numbers ranging from 0.9 to 1.8 and altitudes from 26,000 to 55,000 ft to give a range of unit Reynolds numbers from 1.7 to 4.0 million per ft. Angle of attack was varied from -1° to approximately 10°.

ALPHA   angle of attack, deg

BETA   angle of sideslip, deg

BL   butt line, in.

c   airfoil chord, ft

Cp   pressure coefficient (PL-PSINF)/QBAR

Hp   pressure altitude, ft

IB   inboard row of pressure orifices

L.S.   lower surface

M   Mach number

MINF   free-stream Mach number

OB   outboard row of pressure orifices

PL   local static pressure, lb/ft^2

PSINF   free-stream static pressure, lb/ft^2

QBAR   dynamic pressure, lb/ft^2

Rn   Reynolds number based on free-stream conditions and local chord

Rn_t transition Reynolds number

U.S.   upper surface

x   longitudinal dimension, in.

x/c   nondimensional chord location

x/c_t nondimensional chord location of transition

y   lateral dimension, in.

z   vertical dimension, in.

z/c   nondimensional vertical location

DESCRIPTION OF TEST AIRCRAFT AND WING MODIFICATION

The flight experiment was conducted using an F-15 twin-engine fighter aircraft. The F-15 airplane was chosen for the experiment primarily because of its Mach 2 capability and availability. In addition, previous flight experiments on the F-15 airplane showed that the wing produced a favorable pressure gradient (desirable for obtaining laminar flow) to approximately 25 percent chord. The F-15 aircraft has 45° of leading edge sweep and uses a NACA 64(A)04.6 airfoil at BL 155. Airfoil coordinates at several butt lines are given in table 1. These values do not include the thickness of the wing modification.

A foam and fiberglass cleanup test section was placed on the right wing of the aircraft. Figure 1 shows an in-flight photograph of the F-15 airplane with the foam and fiberglass test section. This near planform view shows the relative location and size of the test section. The intended purpose of the foam and fiberglass test section was to eliminate any possible effects of surface roughness or imperfections. It retained the existing airfoil shape but added approximately 3/16 to 1/4 in. of thickness. This thickness was necessary for the installation of instrumentation plumbing lines. The test section was approximately 4 ft wide, the inboard edge at BL 170 and the outboard edge at BL 218. The aft edge of the test section extended to approximately 30 percent chord on the inboard side and approximately 35 percent chord on the outboard side. The drawing in figure 2 shows the exact location of the test section and the chord values for the inboard and outboard edges of the test section. It had two rows of 15 flush static pressure orifices, one at BL 176, the other at BL 212. The exact chord location of the orifices is given in table 2.

The test section was constructed using one layer of unidirectional fiberglass under 1/8 in. polyurethane foam covered with four layers of bidirectional fiberglass. The surface consisted of body putty and polyester paint. A cross-sectional drawing of the test section is given in figure 3. The waviness of the test section did not exceed 0.0015 in. per 2 in. It was originally painted white but was repainted black towards the end of the experiment to facilitate the use of liquid crystals for flow visualization. In addition, a notch-bump was added to the inboard side of the test section after the sixth flight to eliminate any possible effects of an attachment line transition problem (Gaster, 1965). A photograph of the notch-bump is shown in figure 4.

A potential problem with this construction technique for high altitude and supersonic use was observed after several test flights. Small blisters of approximately 1/16 to 1/8 in. in diameter and approximately 0.002 to 0.010 in. high began to appear in the paint after a flight in which the maximum Mach and altitude were 1.8 and 50,000 ft, respectively. Although the blisters did not break the surface of the paint, they presented an obvious problem for using this construction technique at Mach (M) numbers near 2.0 and above for laminar flow testing. The blisters were caused by gas that was released as the test section was exposed to the higher temperatures caused by flying at supersonic speeds. The origin of the gas is uncertain, but it may have been trapped in the body putty during construction or formed by the resin material during high-temperature exposure. In addition, altitude was considered to aid in the formation of the blisters because of the reduced pressure at altitude resulting in a substantial pressure differential between the trapped gas and the atmosphere.

3

INSTRUMENTATION

Two separate instrumentation systems were used for the flight experiment. Quantities such as free-stream Mach number, pressure altitude, and angle of attack were obtained from the aircraft's main instrumentation system. The main system used two absolute pressure transducers for measuring total and static pressure from the flight test pitot-static probe mounted on a noseboom.

The instrumentation system for the test section consisted of a 32-port, electronically scanned, multiple differential pressure transducer unit, an absolute pressure transducer, and five temperature-compensated hot-film anemometers. The differential pressure transducer unit was used to measure pressures from the two rows of static pressure orifices. The absolute pressure transducer measured the pressure on the reference side of the differential pressure transducer unit. The temperature-compensated hot-film anemometers, similar to the system described in Chiles and Johnson (1985), were used to measure transition location. Temperature-compensated hot-film anemometers were used because changes in ambient, wall, or total temperature can affect the output signal quality of uncompensated hot-film anemometers. The hot-film sensors had a nominal resistance of 12 ohms and the temperature gages had a nominal resistance of 50 ohms. Figure 5 shows a closeup of the hot-film sensor and temperature gage as installed on the test section.

Because only five hot-film anemometers were available on the aircraft, they were relocated from flight to flight to accurately define transition location. The chord locations of the hot film for the various flights of the experiment are given in table 3. The hot-film sensors remained in the 1, 2, 4, 10, and 15 percent chord locations for the entire latter portion of the experiment. Figure 6 shows the hot-film sensors mounted on the test section at 5, 10, 15, 20, and 15 percent chord.

FLOW VISUALIZATION

At several times during the flight test program, attempts were made to use flow visualization as a secondary means of determining transition location. Although no flow visualization results are given, a discussion of the effort is provided to aid future development of flow visualization techniques for supersonic flight. Initially, a mixture of napthalene and red food coloring was used. The red food coloring was added to give greater contrast between the white test section and the napthalene. Only two flights were flown before the napthalene was abandoned because of operational difficulties. The difficulties arose from trying to apply the correct amount of napthalene that would not sublime during the climb and acceleration, but would sublime during the short amount of time (approximately 10 to 20 sec) on test conditions that followed.

After the early portion of flight tests, the test section was painted black to facilitate the use of liquid crystals similar to the technique used in Holmes and others (1986). Pressure sensitive liquid crystals (named by the manufacturer) were used. Operational difficulties were still encountered, however. It was extremely difficult to get the photo chase aircraft in the desired position during supersonic

test runs and was virtually impossible during test points where the test aircraft was in a turn. Because of these difficulties, liquid crystal photos were taken only at low-transonic speeds. An obvious solution would have been to mount a camera on the test aircraft. However, this would have entailed extensive modifications beyond the scope of the project.

TEST CONDITIONS AND MANEUVERS

Test points were flown at Mach numbers ranging between 0.9 and 1.8 at altitudes between 26,000 and 55,000 ft. Mach number and altitude were combined to give a unit Reynolds number range from 1.7 to 4.0 million per ft. Angle of attack ranged from -1° to 10°.

Straight and level points were flown for approximately 20 sec. In order to vary angle of attack, constant g-loading turns were flown. Each constant g-loading condition was held for approximately 10 sec. At the higher Mach numbers and increased g-loading, it was often difficult to maintain both airspeed and altitude, therefore airspeed was given the higher priority. This resulted in some cases where altitude was allowed to decrease to maintain airspeed.

RESULTS AND DISCUSSION

Typical Pressure Distributions

Typical pressure distributions for M = 0.9, 1.2, 1.5, and 1.8 are shown in figure 7. Except for the inboard row at M = 0.9, the pressure distributions show a favorable gradient to approximately 20 percent chord, or greater, for the inboard pressure orifice row. The outboard row indicates a favorable pressure gradient, at least to the aft most orifice, of 33 percent, except for the lower angle-of-attack case at M = 0.9 where the slope became negative near 20 percent chord. An increase in angle of attack increased the pressure measured at the two lower surface orifices as would be expected and decreased the pressure on the upper surface of the test section. At the lower speed cases, M = 0.9 and 1.2, increased angle of attack had a noticeable effect on the shape of the forward portion of the pressure distribution.

These pressure distributions are presented for the typical case. Tabulated pressure coefficients are presented in the appendix for Mach numbers at angles of attack ranging from 1° to 7° but categorized by unit Reynolds numbers of approximately 1.7 and 2.0 million per ft for both the clean and notch-bump configuration. Tabulated pressure coefficients for the higher Reynolds number cases where no laminar flow was detected are not given.

Typical Transition Results

The output from the hot-film anemometers was used to determine boundary layer transition. Figure 8 shows typical outputs from the five anemometers during a test

point at M = 0.9, Hp = 40,600 ft. In figure 8(a) where the angle of attack is 3.3°, the hot-film sensor at 5 percent chord shows an output typical of transitional flow. The other outputs (10, 15, and 20 percent) demonstrate signals typical of turbulent flow. The amplitude of the output for the 10 percent chord anemometer is less than the others, for the same flow condition, because the gain of that particular anemometer was inadvertently set low for several flights.

In figure 8(b) where the angle of attack is 5.0°, the hot films at 5 and 10 percent chord indicate laminar flow. The two gages at 15 percent chord indicate laminar flow with turbulent spikes, and the gage at 20 percent chord indicates periods of transitional flow and turbulent flow with laminar spikes.

At M ≥ 1.2, transition occurred at or very near the leading edge. Figure 9 shows a typical hot-film output for Mach numbers > 1.2. The flight conditions for this point were M = 1.73, Hp = 49,200, ALPHA = 4.5°. All the hot-film gages indicate turbulent flow. Again, the gain on the 10 percent chord hot film was set lower than the others, thus giving the lower amplitude signal. In addition, the inboard 15 percent chord hot film failed early in the flight and was inoperative for this test point. Overall, the temperature-compensated hot-film anemometers worked well for determining transition location throughout the Mach-number range of the experiment.

Summary plots of the most aft that transition occurred, or optimum transition location, are given in figures 10 and 11. Figure 10 presents a plot of optimum transition location as a function of angle of attack for the clean leading-edge configuration at M = 0.9. For this Mach number, the longest runs of laminar flow occurred at 5° and 6° angle of attack. Above 6° and below 5° angle of attack, transition occurred at 5 percent chord or less.

Figure 11 presents optimum transition location as a function of free-stream Mach number for both the clean and notch-bump configurations. Transition occurred at 20 percent chord at M = 0.9 and M = 0.97 for the clean configuration. For the notch-bump configuration at M = 0.9, transition occurred at approximately 15 percent chord. It is important to note that even though the 15 percent chord hot film never indicated pure laminar flow, there were no hot-film gages aft of 15 percent chord to accurately determine transition location. At M = 1.10 (clean configuration) and M = 1.16 (notch-bump configuration), transition occurred at 15 percent chord. At M ≥ 1.2, transition occurred near the leading edge for both leading-edge configurations. It is apparent that the notch-bump had essentially no effect.

The cause of the sharp decrease in optimum transition location and the inability to obtain laminar flow at M > 1.2 is uncertain. But it is important to mention that at the higher Mach numbers (M = 1.2, 1.5, and 1.8), the same angle-of-attack range as at the slower speeds was achieved, therefore eliminating angle of attack as a possibility.

Figure 12 presents transition Reynolds number, based on the optimum transition location, as a function of Mach number. The M = 1.16 test point was obtained with the notch-bump on the leading edge. Transition Reynolds numbers for the optimum cases decreased from approximately 4 million per ft at M = 0.9 to 2 million at M = 1.1 and then increased to 3 million at M = 1.16.

CONCLUDING REMARKS

A preliminary flight experiment was flown to generate a full-scale data base to aid with the assessment of computational codes and improve instrumentation and techniques for measuring boundary layer transition at supersonic speeds.

1. Temperature-compensated hot films worked extremely well for measuring boundary layer transition throughout the Mach range of the experiment.

2. The limit of the foam and fiberglass technique for constructing cleanup test sections or contouring desired airfoils for boundary layer transition experiments appears to be approximately $M = 1.8$ and $Hp = 50,000$ ft because of the occurrence of surface blisters which spoil the original smooth surface.

3. Transition was measured as far aft as 20 percent chord at $M = 0.90$ and $M = 0.97$. At $M = 1.10$ and $M = 1.16$, transition was measured at 15 percent chord. At $M \geqslant 1.20$, transition occurred near the leading edge. Maximum observed transition Reynolds number for this experiment, NACA 64(A)04.6 airfoil with 45° leading-edge sweep, was approximately 4 million per ft.

4. There was no change in optimum transition location (limited to a resolution of 5 percent chord in some cases) with the addition of a notch-bump on the leading edge of the test section.

Ames Research Center
Dryden Flight Research Facility
National Aeronautics and Space Administration
Edwards, California, August 20, 1987.

APPENDIX — TABULATED PRESSURE COEFFICIENTS

Mach (M) = 0.900   Pressure altitude, ft (Hp) = 40,637
  Angle of attack, deg (α) = 3.34   L.S. = lower surface   U.S. = upper surface
  x/c = nondimensional chord location

Inboard row   Outboard row

	x/c, %				x/c, %	
L.S.	1.3	-0.008		L.S.	1.50	-0.309
	0.86	-0.023			1.00	-0.335
	0	Inoperative			0	0.381
U.S.	0.73	-0.341		U.S.	1.00	-0.238
	1.20	-0.458			1.40	-0.342
	3.30	-0.606			3.60	-0.448
	6.20	-0.647			7.00	-0.586
	8.20	-0.589			9.10	-0.625
	10.20	-0.654			11.30	-0.634
	12.60	-0.715			14.00	-0.677
	15.10	-0.783			16.80	-0.711
	17.50	-0.852			19.60	-0.762
	20.10	-0.635			22.40	Inoperative
	25.00	-0.488			22.70	-0.624
	29.80	-0.682			33.00	-0.676

M = 0.897   Hp = 40,580 α = 4.95

Inboard row   Outboard row

	x/c, %				x/c, %	
L.S.	1.3	0.072		L.S.	1.50	-0.043
	0.86	0.199			1.00	0.004
	0	Inoperative			0	0.051
U.S.	0.73	-0.763		U.S.	1.00	-0.644
	1.20	-0.823			1.40	-0.712
	3.30	-0.939			3.60	-0.837
	6.20	-0.975			7.00	-0.901
	8.20	-0.972			9.10	-0.921
	10.20	-1.028			11.30	-0.974
	12.60	-1.064			14.00	-0.991
	15.10	-1.076			16.80	-0.998
	17.50	-1.082			19.60	-1.022
	20.10	-1.041			22.40	Inoperative
	25.00	-1.030			22.70	-1.066
	29.80	-0.908			33.00	-1.127

M= 0.910   Hp = 38,101   α = 2.09

Inboard row   Outboard row

         x/c, %   x/c, %

L.S.   1.3   -0.269   L.S.   1.50   -0.719
        0.86   -0.364   1.00   -0.729
        0   Inoperative   0   0.330
U.S.   0.73   -0.141   U.S.   1.00   -0.066
        1.20   -0.247   1.40   -0.146
        3.30   -0.393   3.60   -0.292
        6.20   -0.514   7.00   -0.447
        8.20   -0.586   9.10   -0.495
        10.20   -0.538   11.30   -0.523
        12.60   -0.487   14.00   -0.561
        15.10   -0.500   16.80   -0.598
        17.50   -0.524   19.60   -0.557
        20.10   -0.542   22.40   Inoperative
        25.00   -0.500   22.70   -0.543
        29.80   -0.632   33.00   -0.637

M = 0.916   Hp = 37,221   α = 5.47

Inboard row   Outboard row

         x/c, %   x/c, %

L.S.   1.3   0.202   L.S.   1.50   0.041
        0.86   0.245   1.00   0.059
        0   Inoperative   0   0.037
U.S.   0.73   -0.756   U.S.   1.00   -0.640
        1.20   -0.797   1.40   -0.724
        3.30   -0.939   3.60   -0.835
        6.20   -0.939   7.00   -0.872
        8.20   -0.947   9.10   -0.947
        10.20   -0.980   11.30   -0.940
        12.60   -1.015   14.00   -0.965
        15.10   -1.064   16.80   -0.988
        17.50   -1.087   19.60   -1.026
        20.10   -1.041   22.40   Inoperative
        25.00   -0.988   22.70   -1.052
        29.80   -1.146   33.00   -1.089

9

M = 1.186   Hp = 45,876   α = 2.00

Inboard row				Outboard row		
	x/c, %				x/c, %	
L.S.	1.3	-0.382		L.S.	1.50	-0.570
	0.86	-0.417			1.00	-0.578
	0	Inoperative			0	0.452
U.S.	0.73	0.136		U.S.	1.00	0.200
	1.20	0.049			1.40	0.144
	3.30	-0.098			3.60	-0.004
	6.20	-0.202			7.00	-0.125
	8.20	-0.220			9.10	-0.180
	10.20	-0.268			11.30	-0.245
	12.60	-0.302			14.00	-0.260
	15.10	-0.373			16.80	-0.317
	17.50	-0.446			19.60	-0.328
	20.10	-0.415			22.40	Inoperative
	25.00	-0.385			22.70	-0.377
	29.80	-0.431			33.00	-0.427

M = 1.198   Hp = 45,638   α = 6.35

Inboard row				Outboard row		
	x/c, %				x/c, %	
L.S.	1.3	0.203		L.S.	1.50	-0.077
	0.86	0.200			1.00	-0.102
	0	Inoperative			0	0.406
U.S.	0.73	-0.193		U.S.	1.00	-0.102
	1.20	-0.261			1.40	-0.171
	3.30	-0.384			3.60	-0.288
	6.20	-0.449			7.00	-0.358
	8.20	-0.481			9.10	-0.421
	10.20	-0.504			11.30	-0.457
	12.60	-0.547			14.00	-0.476
	15.10	-0.565			16.80	-0.517
	17.50	-0.623			19.60	-0.514
	20.10	-0.582			22.40	Inoperative
	25.00	-0.561			22.70	-0.582
	29.80	-0.674			33.00	-0.620

10

M = 1.210   Hp = 41,891   α = 1.42

Inboard row

	x/c, %	
L.S.	1.3	-0.412
	0.86	-0.480
	0	Inoperative
U.S.	0.73	0.194
	1.20	0.109
	3.30	-0.043
	6.20	-0.133
	8.20	-0.187
	10.20	-0.230
	12.60	-0.271
	15.10	-0.333
	17.50	-0.366
	20.10	-0.351
	25.00	-0.347
	29.80	-0.364

Outboard row

	x/c, %	
L.S.	1.50	-0.604
	1.00	-0.600
	0	0.438
U.S.	1.00	0.235
	1.40	0.188
	3.60	0.062
	7.00	-0.078
	9.10	-0.146
	11.30	-0.183
	14.00	-0.224
	16.80	-0.287
	19.60	-0.287
	22.40	Inoperative
	22.70	-0.335
	33.00	-0.385

M = 1.212   Hp = 41,536   α = 4.95

Inboard row

	x/c, %	
L.S.	1.3	0.125
	0.86	0.088
	0	Inoperative
U.S.	0.73	-0.058
	1.20	-0.134
	3.30	-0.252
	6.20	-0.341
	8.20	-0.399
	10.20	-0.400
	12.60	-0.452
	15.10	-0.501
	17.50	-0.472
	20.10	-0.504
	25.00	-0.512
	29.80	-0.602

Outboard row

	x/c, %	
L.S.	1.50	-0.193
	1.00	-0.359
	0	0.476
U.S.	1.00	0.038
	1.40	0.002
	3.60	-0.147
	7.00	-0.255
	9.10	-0.319
	11.30	-0.353
	14.00	-0.386
	16.80	-0.424
	19.60	-0.404
	22.40	Inoperative
	22.70	-0.500
	33.00	-0.516

M = 1.501   Hp = 50,924   α = 2.02

Inboard row				Outboard row		
	x/c, %				x/c, %	
L.S.	1.3	−0.180		L.S.	1.50	−0.202
	0.86	−0.231			1.00	−0.208
	0	Inoperative			0	0.537
U.S.	0.73	0.268		U.S.	1.00	0.328
	1.20	0.206			1.40	0.271
	3.30	0.062			3.60	0.155
	6.20	−0.025			7.00	0.043
	8.20	−0.072			9.10	−0.016
	10.20	−0.087			11.30	−0.052
	12.60	−0.133			14.00	−0.103
	15.10	−0.183			16.80	−0.135
	17.50	−0.224			19.60	−0.152
	20.10	−0.245			22.40	Inoperative
	25.00	−0.231			22.70	−0.197
	29.80	−0.277			33.00	−0.232

M = 1.442   Hp = 50,965   α = 6.94

Inboard row				Outboard row		
	x/c, %				x/c, %	
L.S.	1.3	0.315		L.S.	1.50	0.147
	0.86	0.312			1.00	0.032
	0	Inoperative			0	0.511
U.S.	0.73	−0.024		U.S.	1.00	0.067
	1.20	−0.088			1.40	−0.009
	3.30	−0.174			3.60	−0.092
	6.20	−0.240			7.00	−0.165
	8.20	−0.281			9.10	−0.221
	10.20	−0.296			11.30	−0.237
	12.60	−0.330			14.00	−0.270
	15.10	−0.365			16.80	−0.297
	17.50	−0.392			19.60	−0.325
	20.10	−0.400			22.40	Inoperative
	25.00	−0.355			22.70	−0.360
	29.80	−0.441			33.00	−0.383

M = 1.495   Hp = 46,858   α = 1.28

Inboard row   Outboard row

        x/c, %   x/c, %

L.S.   1.3   -0.334   L.S.   1.50   -0.429
        0.86   -0.281   1.00   -0.458
        0   Inoperative   0   0.530
U.S.   0.73   0.313   U.S.   1.00   0.347
        1.20   0.247   1.40   0.285
        3.30   0.099   3.60   0.172
        6.20   -0.001   7.00   0.068
        8.20   -0.044   9.10   0.022
        10.20   -0.068   11.30   -0.007
        12.60   -0.122   14.00   -0.058
        15.10   -0.163   16.80   -0.100
        17.50   -0.205   19.60   -0.117
        20.10   -0.211   22.40   Inoperative
        25.00   -0.211   22.70   -0.155
        29.80   -0.250   33.00   -0.200

M = 1.458   Hp = 46,414   α = 5.46

Inboard row   Outboard row

        x/c, %   x/c, %

L.S.   1.3   0.193   L.S.   1.50   -0.245
        0.86   0.153   1.00   -0.323
        0   Inoperative   0   0.520
U.S.   0.73   0.037   U.S.   1.00   0.124
        1.20   -0.021   1.40   0.069
        3.30   -0.138   3.60   -0.049
        6.20   -0.213   7.00   -0.126
        8.20   -0.258   9.10   -0.159
        10.20   -0.282   11.30   -0.208
        12.60   -0.325   14.00   -0.238
        15.10   -0.337   16.80   -0.267
        17.50   -0.358   19.60   -0.281
        20.10   -0.353   22.40   Inoperative
        25.00   -0.351   22.70   -0.341
        29.80   -0.434   33.00   -0.371

M = 1.798   Hp = 54,651   α = 1.04

Inboard row

	x/c, %	
L.S.	1.3	-0.229
	0.86	-0.179
	0	Inoperative
U.S.	0.73	0.423
	1.20	0.343
	3.30	0.204
	6.20	0.111
	8.20	0.056
	10.20	0.044
	12.60	-0.011
	15.10	-0.066
	17.50	-0.110
	20.10	-0.118
	25.00	-0.122
	29.80	-0.161

Outboard row

	x/c, %	
L.S.	1.50	-0.317
	1.00	-0.319
	0	0.578
	1.00	0.441
	1.40	0.380
	3.60	0.275
	7.00	0.178
	9.10	0.124
	11.30	0.075
	14.00	0.035
	16.80	-0.007
	19.60	-0.028
	22.40	Inoperative
	22.70	-0.066
	33.00	-0.095

M = 1.759   Hp = 54,100   α = 7.64

Inboard row

	x/c, %	
L.S.	1.3	0.239
	0.86	0.228
	0	Inoperative
U.S.	0.73	0.156
	1.20	0.096
	3.30	-0.009
	6.20	-0.080
	8.20	-0.128
	10.20	-0.161
	12.60	-0.187
	15.10	-0.230
	17.50	-0.244
	20.10	-0.242
	25.00	-0.223
	29.80	-0.294

Outboard row

	x/c, %	
L.S.	1.50	-0.098
	1.00	-0.160
	0	0.585
U.S.	1.00	0.215
	1.40	0.153
	3.60	0.048
	7.00	-0.025
	9.10	-0.062
	11.30	-0.090
	14.00	-0.132
	16.80	-0.161
	19.60	-0.175
	22.40	Inoperative
	22.70	-0.219
	33.00	-0.245

M = 1.796   Hp = 49,029   α = 2.03

Inboard row   Outboard row

         x/c, %   x/c, %

L.S.   1.3   -0.197   L.S.   1.50   -0.301
         0.86   -0.157   1.00   -0.299
         0   Inoperative   0   0.598
U.S.   0.73   0.407   U.S.   1.00   0.430
         1.20   0.344   1.40   0.384
         3.30   0.194   3.60   0.274
         6.20   0.100   7.00   0.169
         8.20   0.049   9.10   0.118
         10.20   0.021   11.30   0.084
         12.60   -0.008   14.00   0.039
         15.10   -0.054   16.80   -0.003
         17.50   -0.096   19.60   -0.022
         20.10   -0.116   22.40   Inoperative
         25.00   -0.110   22.70   -0.066
         29.80   -0.164   33.00   -0.104

M = 1.732   Hp = 49,166   α = 4.51

Inboard row   Outboard row

         x/c, %   x/c, %

L.S.   1.3   -0.116   L.S.   1.50   -0.259
         0.86   -0.058   1.00   -0.270
         0   Inoperative   0   0.609
U.S.   0.73   0.316   U.S.   1.00   0.347
         1.20   0.248   1.40   0.299
         3.30   0.109   3.60   0.189
         6.20   0.015   7.00   0.085
         8.20   -0.030   9.10   0.025
         10.20   -0.060   11.30   0.009
         12.60   -0.095   14.00   -0.033
         15.10   -0.115   16.80   -0.067
         17.50   -0.154   19.60   -0.093
         20.10   -0.174   22.40   Inoperative
         25.00   -0.202   22.70   -0.136
         29.80   -0.223   33.00   -0.161

M = 0.898   Hp = 39,662   α = 3.33
  With notch-bump

Inboard row   Outboard row

        x/c, %   x/c, %

L.S.   1.3   -0.110   L.S.   1.50   -0.506
        0.86   -0.133   1.00   -0.493
        0   Inoperative   0   0.342
U.S.   0.73   -0.319   U.S.   1.00   -0.213
        1.20   -0.415   1.40   -0.297
        3.30   -0.582   3.60   -0.406
        6.20   -0.577   7.00   -0.562
        8.20   -0.650   9.10   -0.599
        10.20   -0.689   11.30   -0.576
        12.60   -0.709   14.00   -0.595
        15.10   -0.625   16.80   -0.644
        17.50   -0.558   19.60   -0.660
        20.10   -0.554   22.40   Inoperative
        25.00   -0.538   22.70   -0.653
        29.80   -0.669   33.00   -0.718

M = 0.882   Hp = 39,331   α = 7.32
  With notch-bump

Inboard row   Outboard row

        x/c, %   x/c, %

L.S.   1.3   0.268   L.S.   1.50   0.146
        0.86   0.320   1.00   0.217
        0   Inoperative   0   -0.498
U.S.   0.73   -1.315   U.S.   1.00   -1.138
        1.20   -1.315   1.40   -1.195
        3.30   -1.258   3.60   -1.266
        6.20   -1.314   7.00   -1.318
        8.20   -1.330   9.10   -1.349
        10.20   -1.354   11.30   -1.327
        12.60   -1.357   14.00   -1.316
        15.10   -1.410   16.80   -1.382
        17.50   -1.411   19.60   -1.342
        20.10   -1.422   22.40   Inoperative
        25.00   -1.311   22.70   -1.009
        29.80   -1.404   33.00   -0.966

16

M = 1.193   Hp = 47,108   α = 2.88
  With notch-bump

Inboard row   Outboard row

         x/c, %   x/c, %

L.S.   1.3   -0.344   L.S.   1.50   -0.327
       0.86   -0.392   1.00   -0.310
       0   Inoperative   0   0.480
U.S.   0.73   0.098   U.S.   1.00   0.159
       1.20   0.007   1.40   0.094
       3.30   -0.159   3.60   -0.030
       6.20   -0.243   7.00   -0.163
       8.20   -0.306   9.10   -0.240
      10.20   -0.301   11.30   -0.263
      12.60   -0.355   14.00   -0.311
      15.10   -0.411   16.80   -0.327
      17.50   -0.450   19.60   -0.325
      20.10   -0.493   22.40   Inoperative
      25.00   -0.436   22.70   -0.408
      29.80   -0.484   33.00   -0.467

M = 1.157   Hp = 45,380   α = 8.60
  With notch-bump

Inboard row   Outboard row

         x/c, %   x/c, %

L.S.   1.3   0.325   L.S.   1.50   0.163
       0.86   0.353   1.00   0.181
       0   Inoperative   0   0.235
U.S.   0.73   -0.432   U.S.   1.00   -0.329
       1.20   -0.459   1.40   -0.392
       3.30   -0.571   3.60   -0.506
       6.20   -0.633   7.00   -0.554
       8.20   -0.645   9.10   -0.594
      10.20   -0.675   11.30   -0.622
      12.60   -0.702   14.00   -0.640
      15.10   -0.737   16.80   -0.664
      17.50   -0.776   19.60   -0.670
      20.10   -0.773   22.40   Inoperative
      25.00   -0.703   22.70   -0.722
      29.80   -0.783   33.00   -0.756

M = 1.472   Hp = 50,311   α = 1.81
   With notch-bump

Inboard row   Outboard row

         x/c, %   x/c, %

L.S.   1.3   -0.201   L.S.   1.50   -0.174
        0.86   -0.218   1.00   -0.170
        0   Inoperative   0   0.553
U.S.   0.73   0.281   U.S.   1.00   0.327
        1.20   0.209   1.40   0.270
        3.30   0.059   3.60   0.167
        6.20   -0.038   7.00   0.044
        8.20   -0.082   9.10   0.004
       10.20   -0.097   11.30   -0.047
       12.60   -0.129   14.00   -0.089
       15.10   -0.174   16.80   -0.131
       17.50   -0.226   19.60   -0.143
       20.10   -0.243   22.40   Inoperative
       25.00   -0.238   22.70   -0.207
       29.80   -0.265   33.00   -0.243

M = 1.405   Hp = 50,765   α = 8.18
   With notch-bump

Inboard row   Outboard row

         x/c, %   x/c, %

L.S.   1.3   0.334   L.S.   1.50   0.181
        0.86   0.364   1.00   0.147
        0   Inoperative   0   0.429
U.S.   0.73   -0.137   U.S.   1.00   -0.048
        1.20   -0.185   1.40   -0.123
        3.30   -0.298   3.60   -0.227
        6.20   -0.353   7.00   -0.275
        8.20   -0.383   9.10   -0.322
       10.20   -0.405   11.30   -0.340
       12.60   -0.434   14.00   -0.373
       15.10   -0.467   16.80   -0.395
       17.50   -0.483   19.60   -0.409
       20.10   -0.493   22.40   Inoperative
       25.00   -0.447   22.70   -0.445
       29.80   -0.486   33.00   -0.480

18

M = 1.669   Hp = 54,508   α = 7.94
With notch-bump

Inboard row   Outboard row

       x/c, %   x/c, %

L.S.   1.3   0.262   L.S.   1.50   0.041
       0.86   0.297   1.00   0.017
       0   Inoperative   0   0.533
U.S.   0.73   0.072   U.S.   1.00   0.116
       1.20   0.017   1.40   0.091
       3.30   -0.101   3.60   -0.028
       6.20   -0.157   7.00   -0.093
       8.20   -0.200   9.10   -0.129
       10.20   -0.223   11.30   -0.171
       12.60   -0.257   14.00   -0.186
       15.10   -0.283   16.80   -0.233
       17.50   -0.308   19.60   -0.258
       20.10   -0.310   22.40   Inoperative
       25.00   -0.275   22.70   -0.271
       29.80   -0.346   33.00   -0.291

M = 1.715   Hp = 54,577   α = 1.30
With notch-bump

Inboard row   Outboard row

       x/c, %   x/c, %

L.S.   1.3   -0.288   L.S.   1.50   -0.381
       0.86   -0.224   1.00   -0.395
       0   Inoperative   0   0.526
U.S.   0.73   0.344   U.S.   1.00   0.373
       1.20   0.277   1.40   0.313
       3.30   0.130   3.60   0.212
       6.20   0.047   7.00   0.101
       8.20   -0.019   9.10   0.055
       10.20   -0.032   11.30   0.027
       12.60   -0.058   14.00   -0.029
       15.10   -0.127   16.80   -0.071
       17.50   -0.153   19.60   -0.090
       20.10   -0.176   22.40   Inoperative
       25.00   -0.179   22.70   -0.140
       29.80   -0.218   33.00   -0.172

M = 1.193   Hp = 41,931   α = 1.09
  With notch-bump

Inboard row   Outboard row

        x/c, %   x/c, %

L.S.   1.3   -0.436   L.S.   1.50   -0.367
        0.86   -0.495   1.00   -0.364
        0   Inoperative   0   0.445
U.S.   0.73   0.188   U.S.   1.00   0.260
        1.20   0.115   1.40   0.192
        3.30   -0.047   3.60   0.062
        6.20   -0.131   7.00   -0.077
        8.20   -0.200   9.10   -0.137
        10.20   -0.229   11.30   -0.180
        12.60   -0.281   14.00   -0.232
        15.10   -0.329   16.80   -0.274
        17.50   -0.346   19.60   -0.287
        20.10   -0.349   22.40   Inoperative
        25.00   -0.339   22.70   -0.352
        29.80   -0.367   33.00   -0.369

M = 1.182   Hp = 41.533   α = 5.24
  With notch-bump

Inboard row   Outboard row

        x/c, %   x/c, %

L.S.   1.3   0.136   L.S.   1.50   -0.209
        0.86   0.137   1.00   -0.215
        0   Inoperative   0   0.451
U.S.   0.73   -0.134   U.S.   1.00   -0.067
        1.20   -0.240   1.40   -0.101
        3.30   -0.372   3.60   -0.214
        6.20   -0.412   7.00   -0.332
        8.20   -0.469   9.10   -0.404
        10.20   -0.479   11.30   -0.445
        12.60   -0.501   14.00   -0.456
        15.10   -0.551   16.80   -0.509
        17.50   -0.540   19.60   -0.494
        20.10   -0.570   22.40   Inoperative
        25.00   -0.563   22.70   -0.545
        29.80   -0.637   33.00   -0.577

20

M = 1.493   Hp = 47,021   α = 1.11
  With notch-bump

Inboard row   Outboard row

        x/c, %   x/c, %

L.S.   1.3   -0.235   L.S.   1.50   -0.204
        0.86   -0.270   1.00   -0.217
        0   Inoperative   0   0.549
U.S.   0.73   0.345   U.S.   1.00   0.367
        1.20   0.259   1.40   0.309
        3.30   0.117   3.60   0.200
        6.20   0.011   7.00   0.081
        8.20   -0.035   9.10   0.028
        10.20   -0.056   11.30   -0.010
        12.60   -0.102   14.00   -0.041
        15.10   -0.156   16.80   -0.092
        17.50   -0.202   19.60   -0.118
        20.10   -0.208   22.40   Inoperative
        25.00   -0.213   22.70   -0.167
        29.80   -0.247   33.00   -0.205

M = 1.478   Hp = 46,098   α = 5.57
  With notch-bump

Inboard row   Outboard row

        x/c, %   x/c, %

L.S.   1.3   0.181   L.S.   1.50   -0.227
        0.86   0.186   1.00   -0.271
        0   Inoperative   0   0.511
U.S.   0.73   0.062   U.S.   1.00   0.127
        1.20   0.011   1.40   0.063
        3.30   -0.101   3.60   -0.035
        6.20   -0.185   7.00   -0.121
        8.20   -0.243   9.10   -0.164
        10.20   -0.270   11.30   -0.203
        12.60   -0.303   14.00   -0.236
        15.10   -0.339   16.80   -0.267
        17.50   -0.358   19.60   -0.313
        20.10   -0.350   22.40   Inoperative
        25.00   -0.340   22.70   -0.327
        29.80   -0.408   33.00   -0.352

REFERENCES

Banner, R.D.; McTigue, J.G.; and Petty, Gilbert, Jr.: Boundary-Layer Transition in Full-Scale Flight. NACA Conference on High-Speed Aerodynamics, Mar. 1958.

Chiles, H.R.; and Johnson, J.B.: Development of a Temperature-Compensated Hot-Film Anemometer System for Boundary-Layer Transition Detection on High-Performance Aircraft. NASA TM-86732, 1985.

Fisher, D.F.; and Dougherty, N.S., Jr.: In-Flight Transition Measurement on a 10° Cone at Mach Numbers From 0.5 to 2.0. NASA TP-1971, 1982.

Gaster, M: A Simple Device for Preventing Turbulent Contamination on Swept Leading Edges. Royal Aero. Soc. J. Technical Notes, vol. 69, Nov. 1965, pp. 788-789.

Holmes, B.J.; Gall, P.D.; Croom, C.C.; Manuel, G.S.; and Kelliher, W.C.: A New Method for Laminar Boundary Layer Transition Visualization in Flight — Color Changes in Liquid Crystal Coatings. NASA TM-87666, 1986.

McTigue, J.G.; Overton, J.D.; and Petty, Gilbert, Jr.: Two Techniques for Detecting Boundary-Layer Transition in Flight at Supersonic Speeds and at Altitudes Above 20,000 Feet. NASA TN D-18, 1959.

Meyer, R.R.; Trujillo, B.M.; and Bartlett, D.W.: F-14 VSTFE and Results of the Cleanup Flight Test Program. Presented at Research in Natural Laminar Flow and Laminar-Flow Control Symposium, Langley Research Center, Hampton, Virginia, Mar. 1987. NASA CP-2487, Part 2, 1987.

Runyan, L.J.; Navran, B.H.; and Rozendaal, R.A.: F-111 Natural Laminar Flow Glove Flight Test Data Analysis and Boundary Layer Stability Analysis. NASA CR-166051, 1984.

TABLE 1. — F-15 AIRFOIL COORDINATES
Butt line (BL) 160 in.

Upper surface		Lower surface	
x/c	z/c	x/c	z/c
0.00000000	0.00000000	0.00000000	0.00000000
0.00059247	0.00204976	0.00140765	-0.00159829
0.00223626	0.00415909	0.00376388	-0.00281839
0.00415688	0.00503680	0.00584315	-0.00282515
0.00888825	0.00761491	0.01111231	-0.00330331
0.02854337	0.01469216	0.03145677	-0.00300669
0.04855364	0.01979557	0.05144643	-0.00218559
0.09894502	0.02850951	0.10105463	-0.00095231
0.14937433	0.03381859	0.15062629	-0.00103670
0.19967105	0.03716926	0.20032923	-0.00184030
0.24982642	0.03931962	0.25017399	-0.00278309
0.29987906	0.04068059	0.30012100	-0.00347595
0.34988075	0.04145605	0.35011938	-0.00371327
0.39987320	0.04172819	0.40012700	-0.00343121
0.44988255	0.04151548	0.45011780	-0.00266167
0.49991540	0.04081573	0.50008453	-0.00148894
0.54996425	0.03963478	0.55003582	-0.00001655
0.60001482	0.03800423	0.59998531	0.00165827
0.65005312	0.03598742	0.64994708	0.00346009
0.70007212	0.03367442	0.69992774	0.00533976
0.75007340	0.03116691	0.74992654	0.00726948
0.80006502	0.02855171	0.79993498	0.00922871
0.85005878	0.02586397	0.84994095	0.01117663
0.90006005	0.02303923	0.89993974	0.01301631
0.95005843	0.01985590	0.94994184	0.01454806
0.98004020	0.01759840	0.97995980	0.01517715
0.99002727	0.01675709	0.98997252	0.01531408
1.00000000	0.01564020	1.00000000	0.01564020

TABLE 1. — Continued.

BL 190

Upper surface		Lower surface	
x/c	z/c	x/c	z/c
0.00000000	0.00000000	0.00000000	0.00000000
0.00067135	0.00156582	0.00132907	-0.00106342
0.00236780	0.00332090	0.00363288	-0.00182660
0.00427904	0.00422124	0.00572149	-0.00175277
0.00900515	0.00672067	0.01099542	-0.00188968
0.02852992	0.01425356	0.03147031	-0.00095004
0.04840646	0.02008026	0.05159383	0.00030198
0.09859657	0.03057650	0.10140343	0.00270596
0.14896463	0.03729205	0.15103566	0.00401942
0.19927878	0.04163773	0.20072172	0.00467128
0.24949614	0.04444756	0.25050465	0.00505683
0.29963588	0.04622552	0.30036462	0.00543685
0.34973020	0.04725856	0.35027050	0.00594808
0.39980801	0.04769324	0.40019257	0.00663941
0.44988623	0.04758969	0.45011455	0.00750201
0.49996751	0.04696607	0.50003299	0.00850168
0.55004672	0.04582800	0.54995349	0.00959863
0.60011338	0.04419414	0.59988662	0.01076437
0.65015840	0.04210338	0.64984139	0.01198460
0.70017766	0.03962178	0.69982283	0.01325794
0.75017323	0.03683325	0.74982698	0.01458428
0.80015425	0.03382498	0.79984624	0.01594316
0.85013115	0.03066279	0.84986905	0.01726522
0.90010962	0.02735675	0.89989087	0.01839107
0.95008305	0.02381999	0.94991674	0.01902732
0.98005690	0.02149488	0.97994303	0.01897901
0.99004480	0.02066853	0.98995512	0.01885944
1.00000000	0.01924987	1.00000000	0.01924987

TABLE 2. — CHORDWISE PRESSURE ORIFICE LOCATIONS

Identification no.		Inboard row, % (C = 137.3 in.)	Outboard row, % (C = 99.4 in.)
L.S.	1	1.3	1.5
	2	0.86	1.0
	3	0*	0
U.S.	4	0.73	1.0
	5	1.2	1.4
	6	3.3	3.6
	7	6.2	7.0
	8	8.2	9.1
	9	10.2	11.3
	10	12.6	14.0
	11	15.1	16.8
	12	17.5	19.6
	13	20.1	22.4*
	14	25.0	27.7
	15	29.8	33.0

*Pressure orifice inoperative.

TABLE 3. — HOT-FILM SENSOR LOCATIONS

Flight no.	Location (% chord)				
	No.1, outboard	No. 2	No. 3	No. 4	No. 5, inboard
463	5	10	15	20	25
464	5	10	15	20	15
465	5	10	15	20	15
466	5	10	15	20	15
467	5	10	15	20	15
468	0	2	4	10	15
469	1	2	4	10	15
470	1	2	4	10	15
471	1	2	4	10	15

TABLE 1. — Concluded.

BL 210

Upper surface		Lower surface	
x/c	z/c	x/c	z/c
0.00000000	0.00000000	0.00000000	0.00000000
0.00064038	0.00168623	0.00135993	-0.00118319
0.00231698	0.00351105	0.00368273	-0.00201224
0.00423460	0.00437767	0.00576508	-0.00189731
0.00896232	0.00684125	0.01103770	-0.00196541
0.02850404	0.01416007	0.03149631	-0.00049245
0.04837015	0.01989854	0.05162958	0.00141087
0.09846401	0.03079307	0.10153612	0.00549372
0.14873490	0.03846843	0.15126439	0.00831183
0.19900694	0.04397168	0.20099323	0.01018376
0.24923596	0.04789334	0.25076404	0.01149391
0.29942119	0.05060329	0.30057854	0.01253994
0.34957334	0.05233683	0.35042737	0.01351731
0.39970335	0.05324466	0.40029652	0.01453549
0.44981991	0.05342474	0.45017969	0.01563694
0.49992665	0.05294707	0.50007335	0.01682052
0.55002118	0.05186946	0.54997864	0.01805579
0.60009874	0.05025124	0.59990140	0.01930069
0.65015540	0.04815602	0.64984456	0.02050916
0.70018880	0.04565582	0.69981157	0.02163780
0.75019882	0.04282512	0.74980118	0.02264740
0.80019082	0.03973165	0.79980958	0.02349829
0.85017003	0.03642500	0.84983010	0.02414459
0.90013943	0.03291567	0.89986053	0.02451810
0.95009594	0.02915301	0.94990385	0.02451409
0.98005892	0.02671957	0.97994075	0.02426400
0.99004401	0.02586887	0.98995607	0.02412866
1.00000000	0.02448176	1.00000000	0.02448176
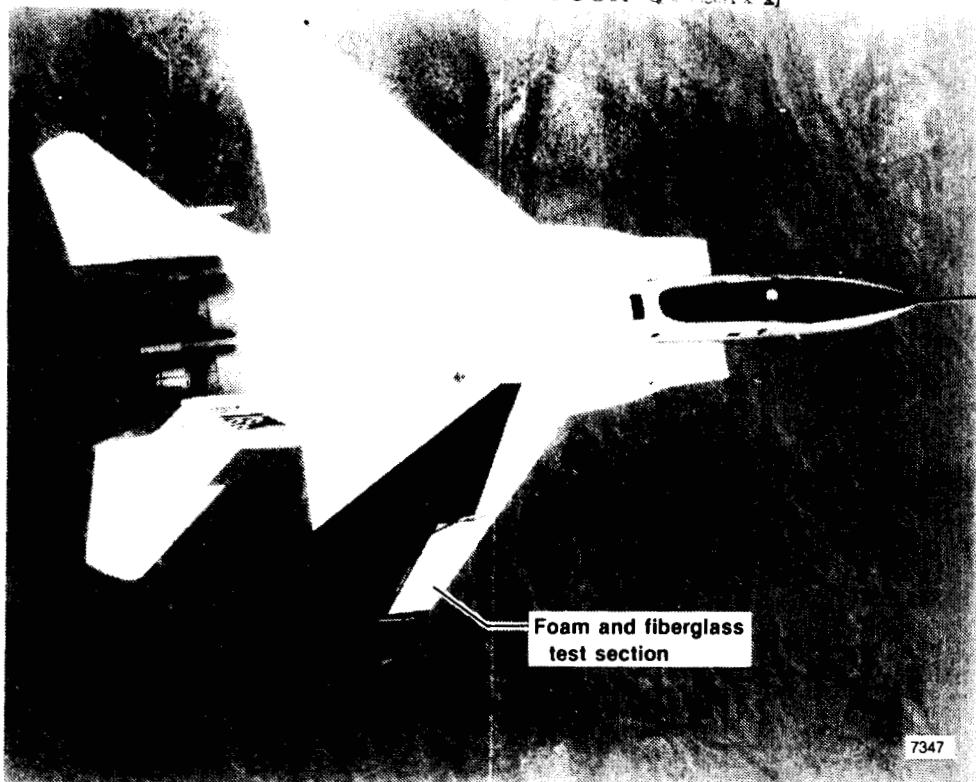
Figure 1. In-flight photograph of F-15 aircraft with foam and fiberglass test section.

Chord Dimensions
Inboard (C1) = 149.0 in.
Outboard (C2) = 111.5 in.

8 ft 11 in. —BL 170

Static
pressure
orifices—

11 ft 6 in. —BL 218

Test
section—

C1

C2

—Extends back to
approximately
33 percent
chord

Not to scale |←— 4 ft —→|

7348
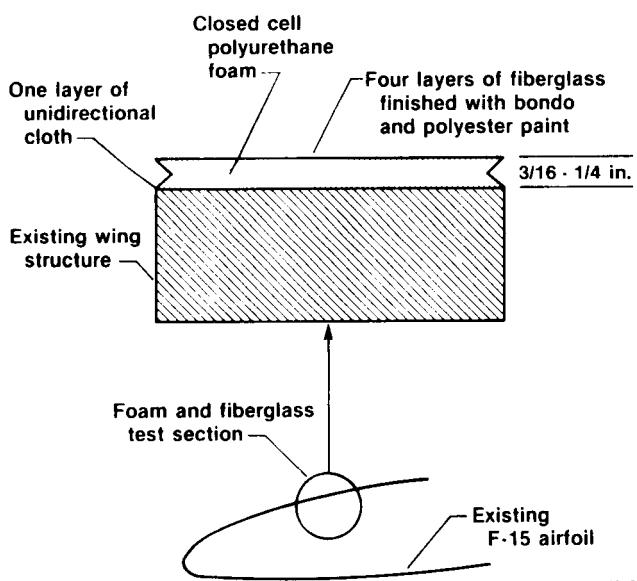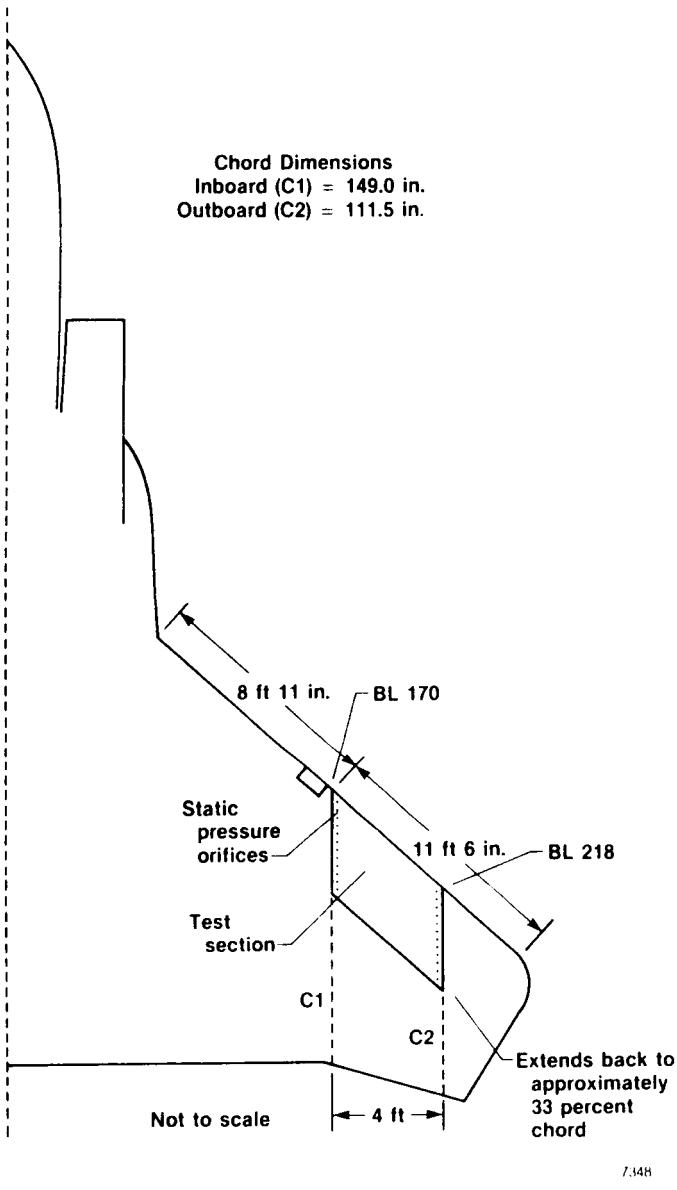
Figure 2. Location of foam and fiberglass test section.

Closed cell
polyurethane
foam —

One layer of
unidirectional
cloth —

—Four layers of fiberglass
finished with bondo
and polyester paint

3/16 · 1/4 in.

Existing wing
structure —

Foam and fiberglass
test section —

—Existing
F-15 airfoil

7349

Figure 3. Schematic of F-15 aircraft test section construction.

Inboard ⟶

7350
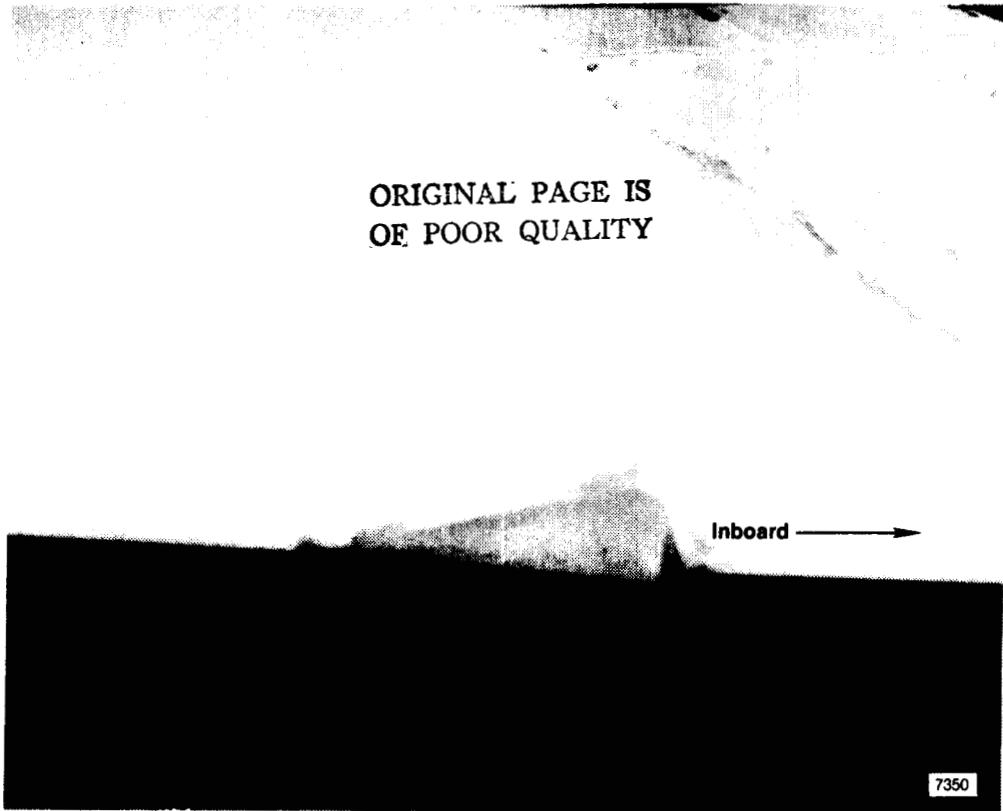
Figure 4. Notch-bump on inboard leading edge of test section.
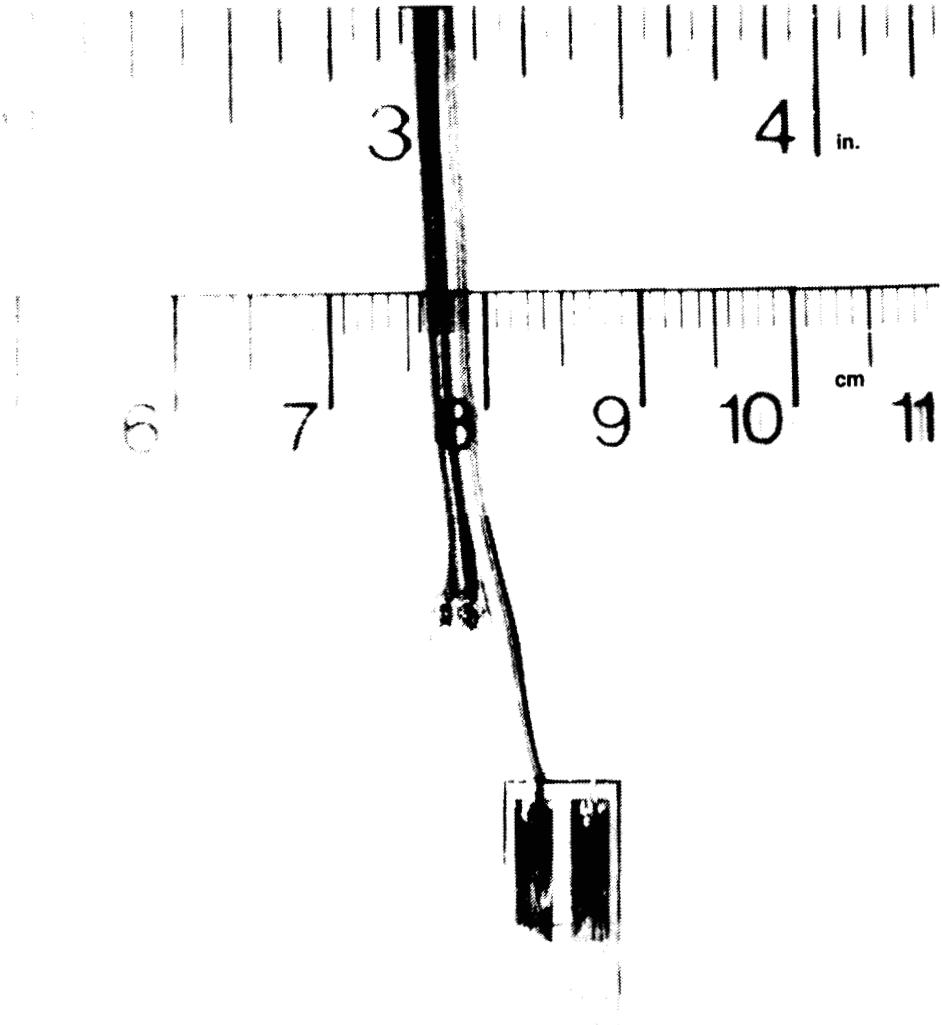
7351

Figure 5. Closeup of typical hot-film sensor and temperature gage installation.

Leading edge

7352
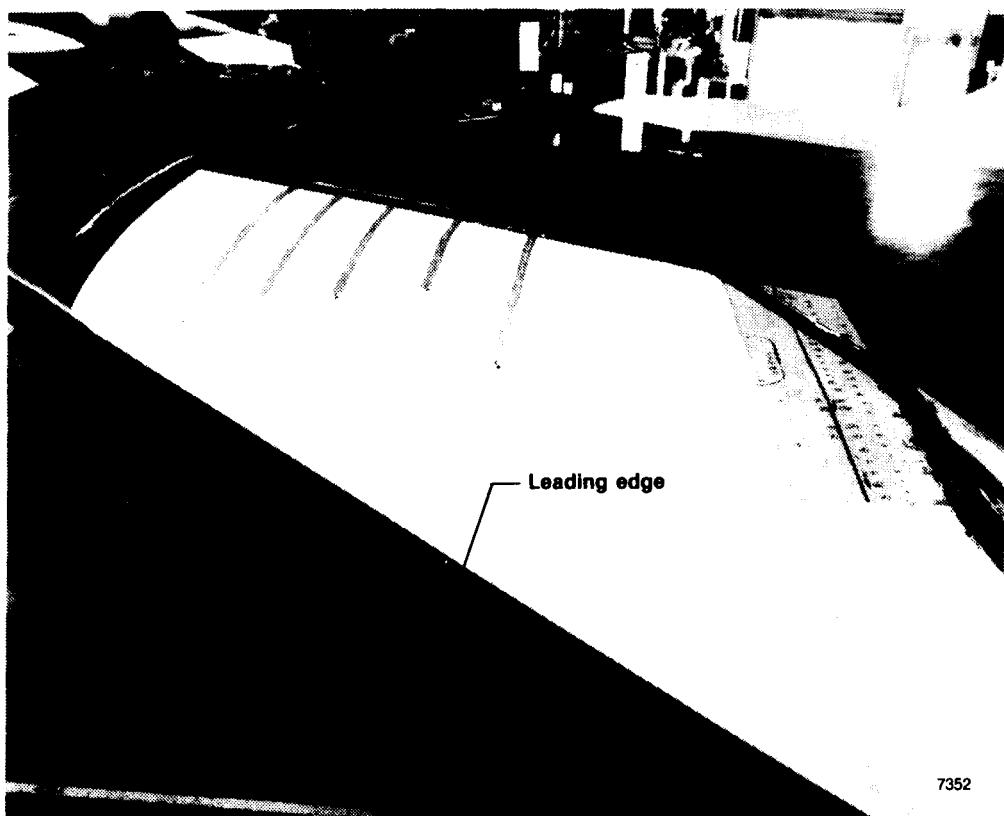
Figure 6. *Hot-film sensors mounted on tes_ section prior to notch-bump installation.*
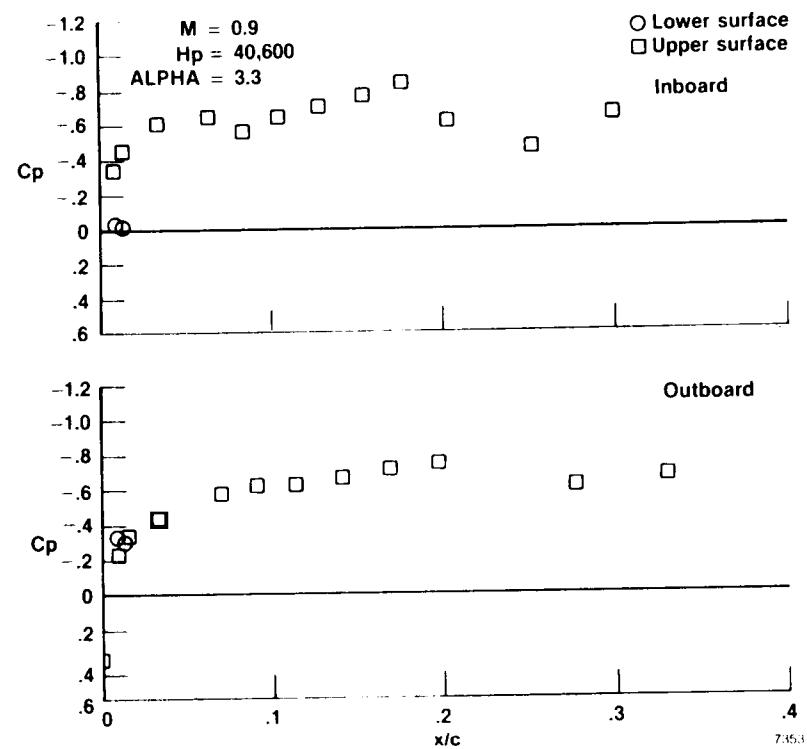
Figure 7. Typical pressure distributions.
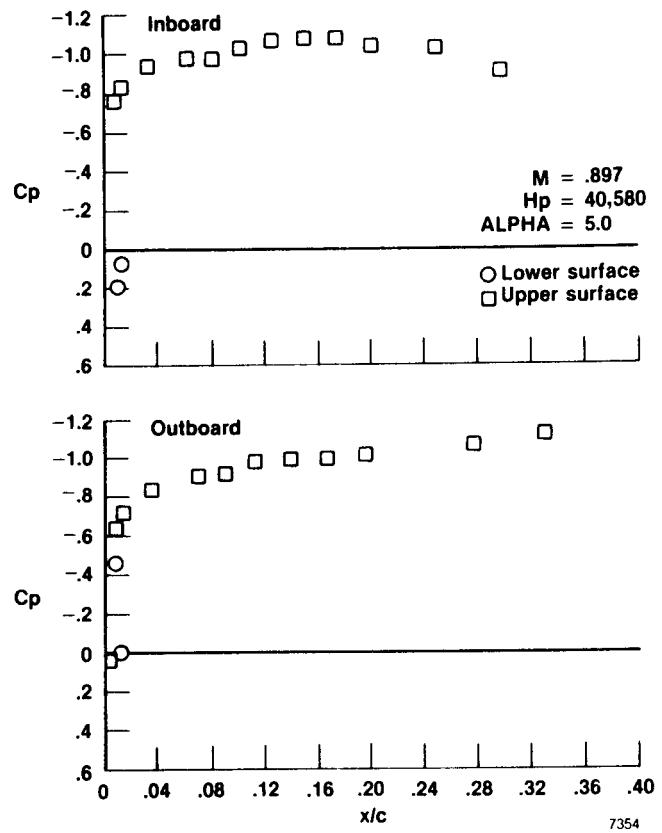
(b)

Figure 7. Continued.
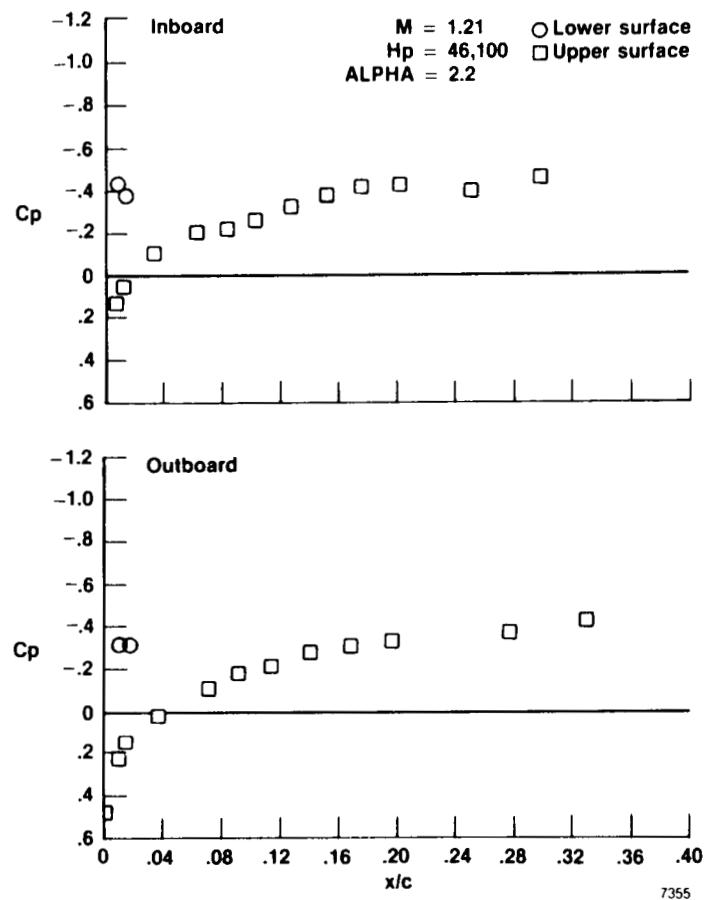
(c)

Figure 7. Continued.

(d)
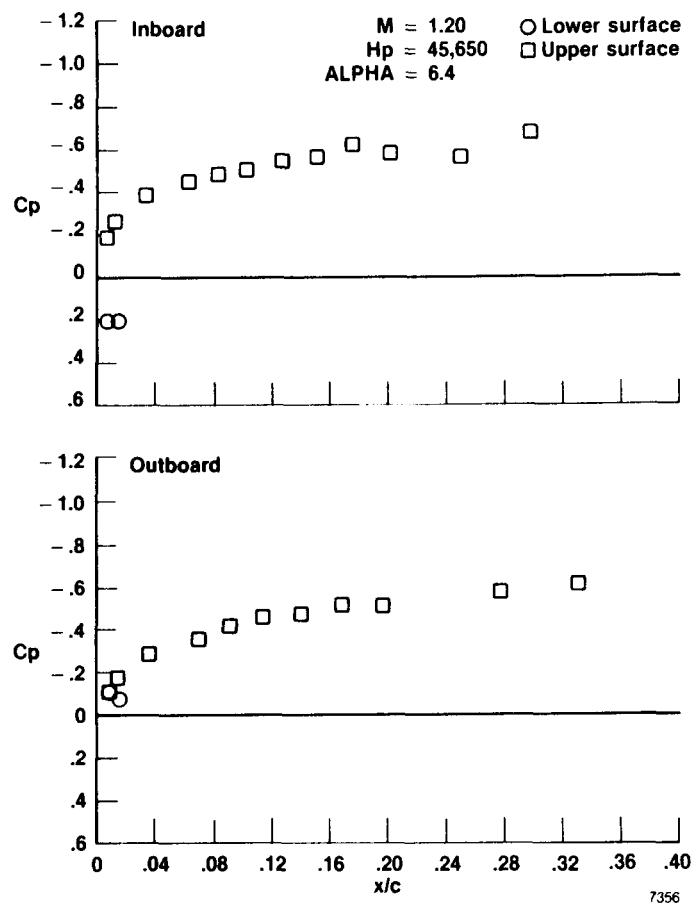
Figure 7. Continued.
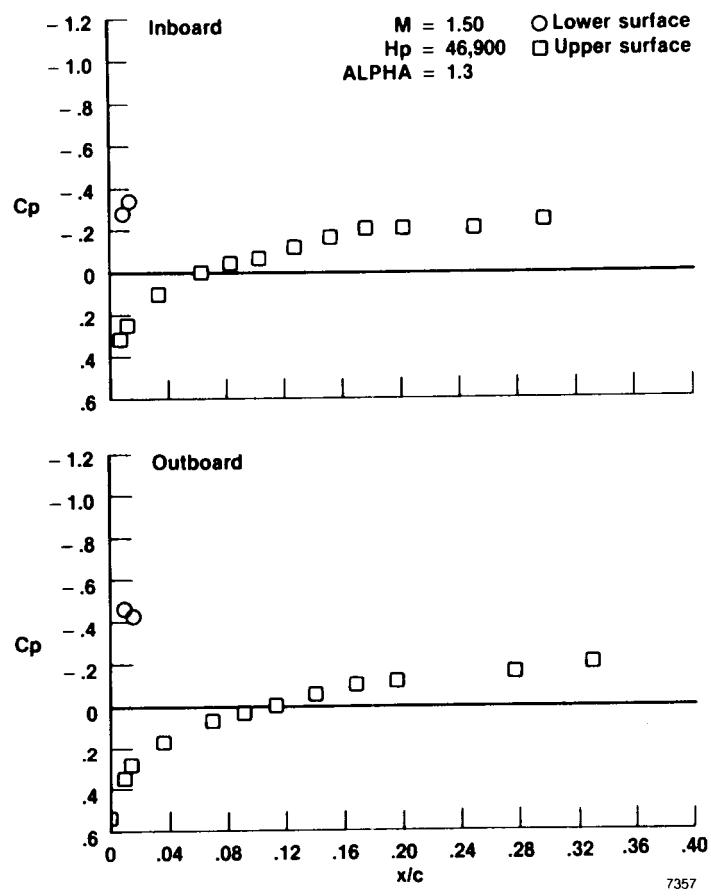
(e)

Figure 7. Continued.
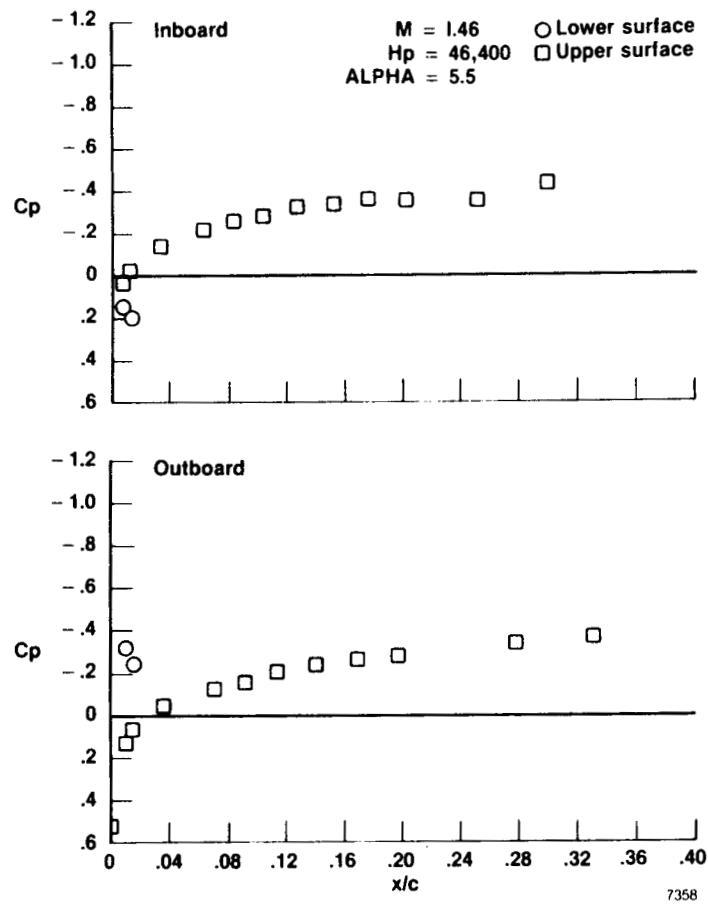
Figure 7. Continued.
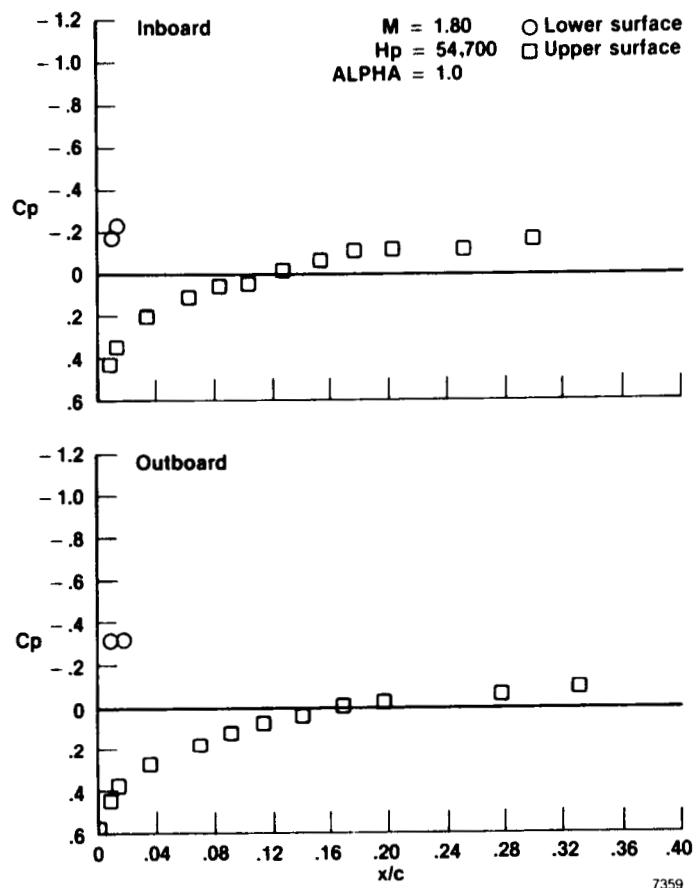
(g)

Figure 7. Continued.
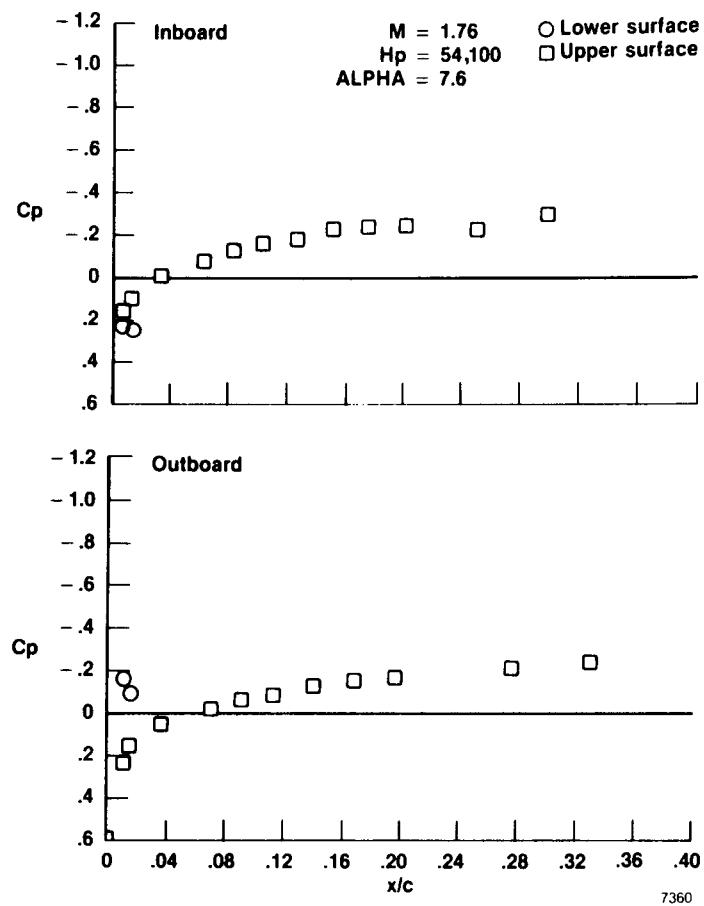
(h)

Figure 7.   Concluded.
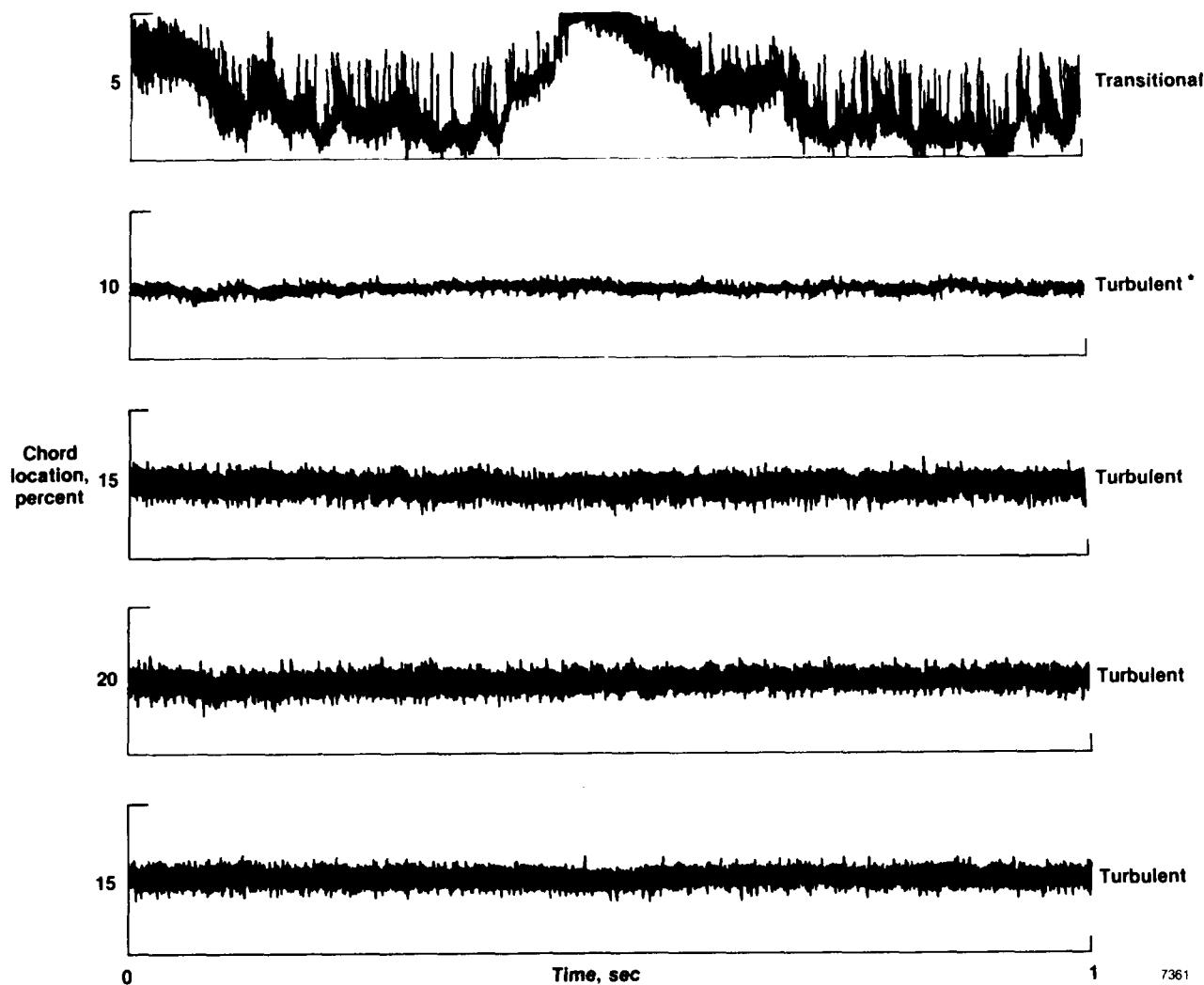
(a) Alpha = 3.3°; *low-gain setting.

Figure 8. Typical hot-film output. M = 0.9, Hp = 40,600 ft.
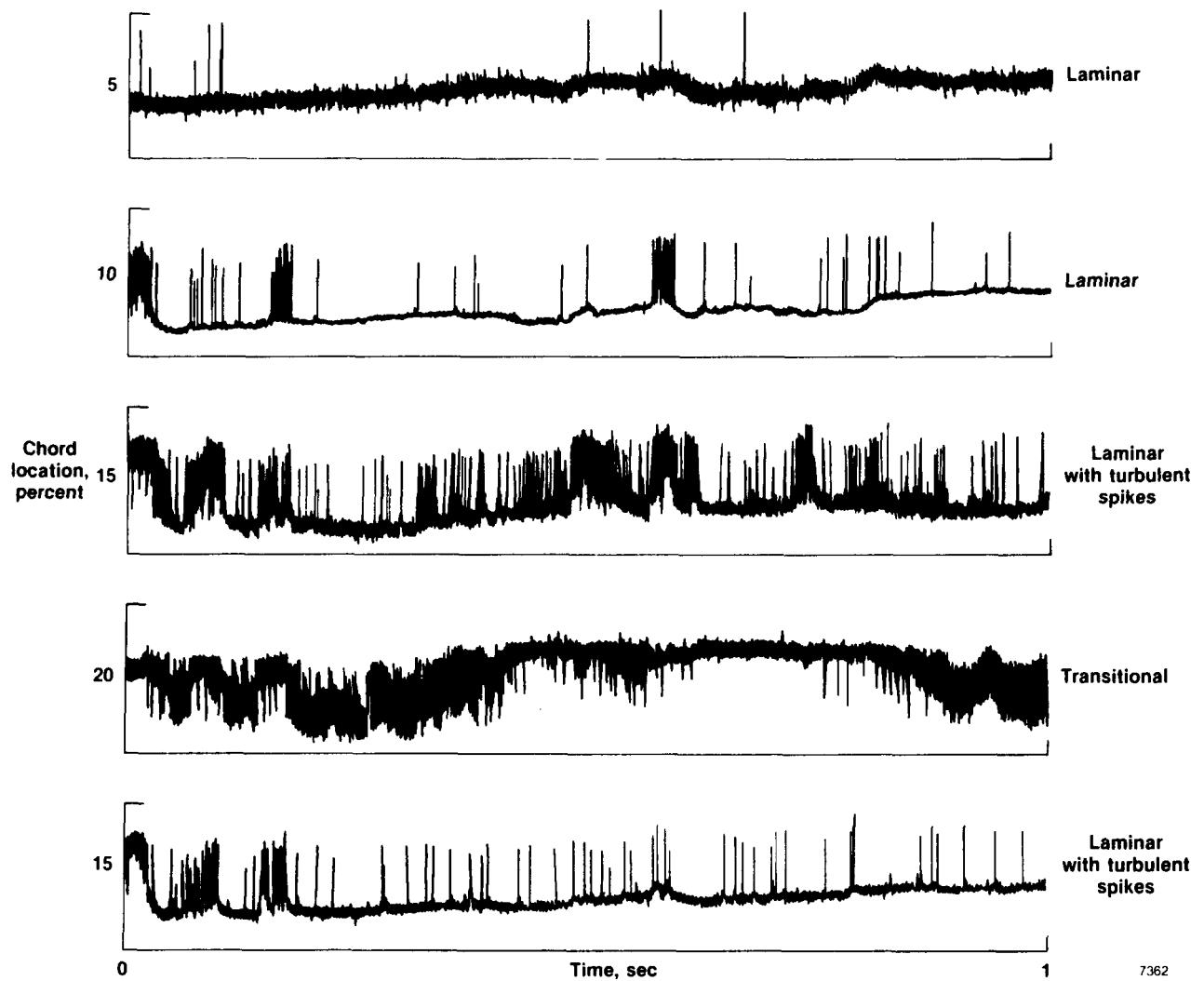
(b)   Alpha = 5.0°.

Figure 8.   Concluded.
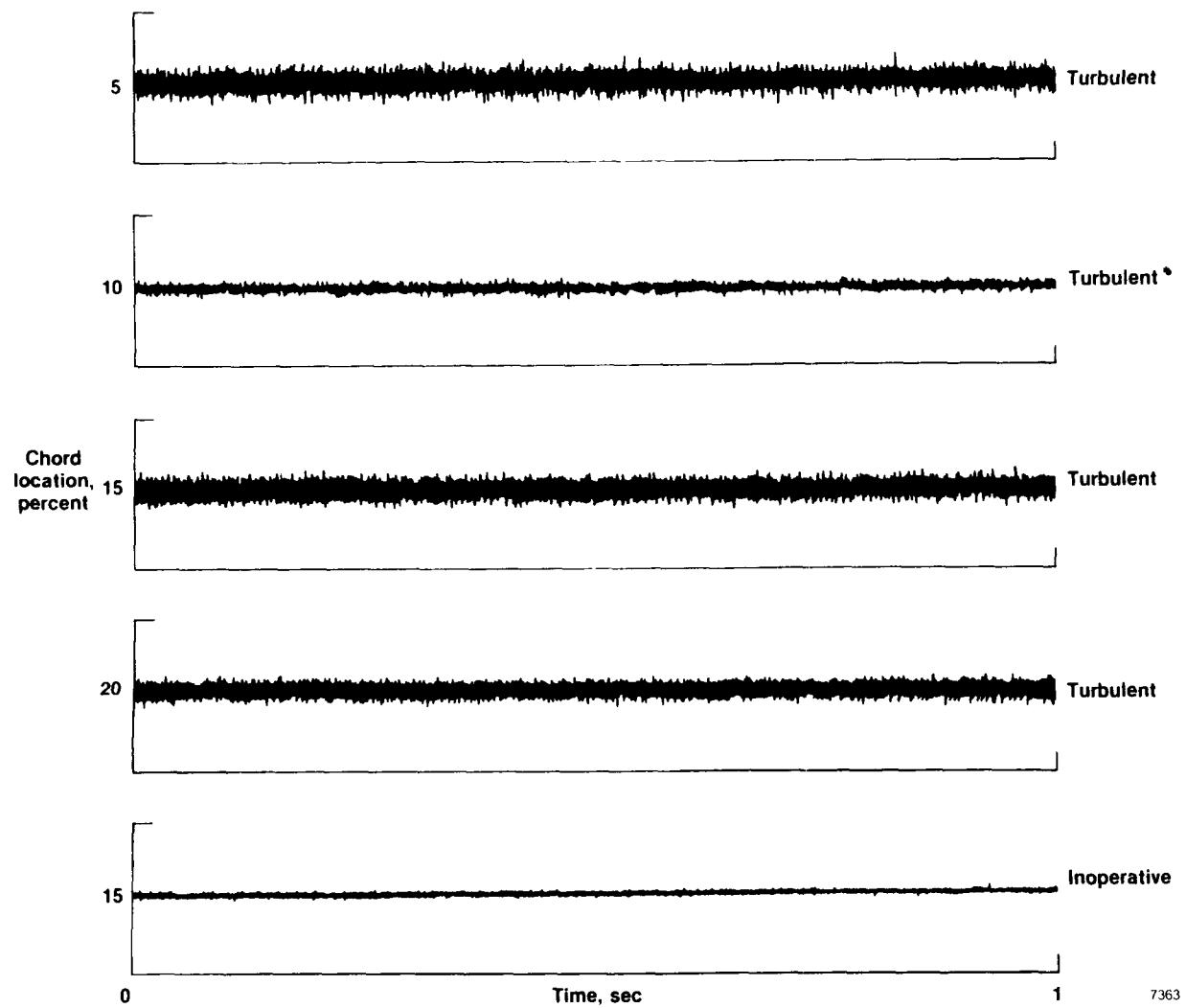
Figure 9. Typical hot-film output. $M = 1.73$, $Hp = 49,200$ ft, $\alpha = 4.5°$.
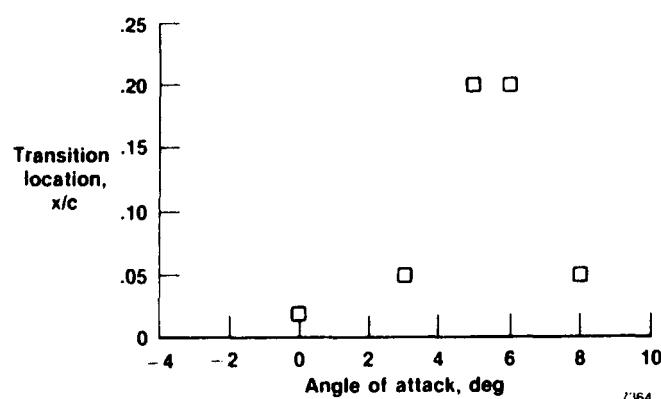
Figure 10. Optimum transition location as a function of angle of attack. Clean configuration. M = 0.9, Hp = 40,000 ft.
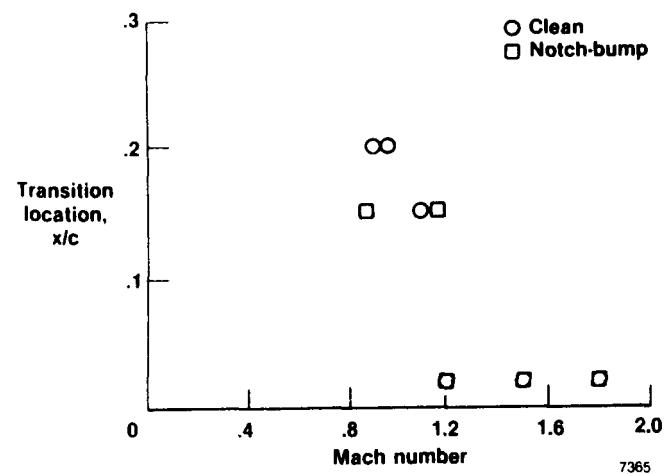
Figure 11. Optimum transition location as a function of Mach number.
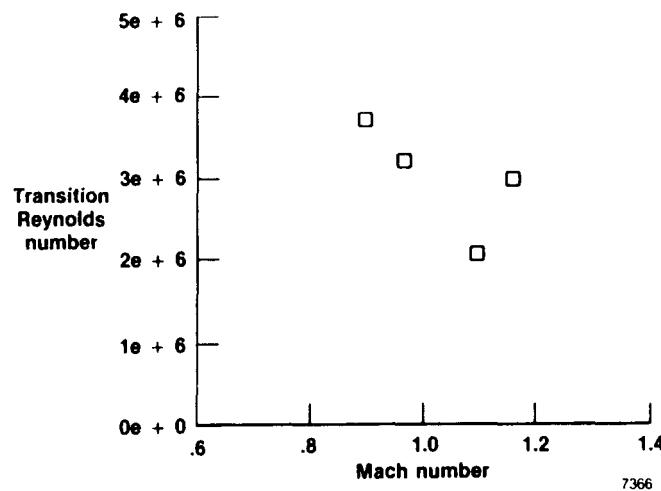
Figure 12. Transition Reynolds number as a function of Mach number.

Report Documentation Page

1. Report No. NASA TM-100412	2. Government Accession No.	3. Recipient's Catalog No.

4. Title and Subtitle	5. Report Date
Preliminary In-Flight Boundary Layer Transition Measurements on a 45-Degree Swept Wing at Mach Numbers Between 0.9 and 1.8	March 1988
	6. Performing Organization Code

7. Author(s)	8. Performing Organization Report No.
J. Blair Johnson	H-1436
	10. Work Unit No. RTOP 533-02-21

9. Performing Organization Name and Address	11. Contract or Grant No.
NASA Ames Research Center Dryden Flight Research Facility P.O. Box 273 Edwards, CA 93523-5000	13. Type of Report and Period Covered

12. Sponsoring Agency Name and Address	13. Type of Report and Period Covered Technical Memorandum
National Aeronautics and Space Administration Washington, DC 20546	14. Sponsoring Agency Code

15. Supplementary Notes

16. Abstract

A preliminary flight experiment was flown to generate a full-scale supersonic data base to aid the assessment of computational codes, to improve instrumentation for measuring boundary layer transition at supersonic speeds, and to provide preliminary information for the definition of follow-on programs. The experiment was conducted using an F-15 aircraft that was modified with a small cleanup test section on the right wing. Results are presented for Mach (M) numbers from 0.9 to 1.8 at altitudes from 26,000 to 55,000 ft. At $M > 1.2$, transition occurred near or at the leading edge for the clean configuration. The furthest aft that transition was measured was 20 percent chord at $M = 0.9$ and $M = 0.97$. No change in transition location was observed after the addition of a notch-bump on the leading edge of the inboard side of the test section which was intended to minimize attachment line transition problems. Some flow visualization was attempted during the flight experiment with both subliming chemicals and liquid crystals. However, difficulties arose from the limited time the test aircraft was able to hold test conditions and the difficulty of positioning the photo chase aircraft during supersonic test points. Therefore, no supersonic transition results were obtained using flow visualization.

17. Key Words (Suggested by Author(s))	18. Distribution Statement
Supersonic laminar flow Laminar flow Natural laminar flow	Unclassified — Unlimited Subject category 34

19. Security Classif. (of this report)	20. Security Classif. (of this page)	21. No. of pages	22. Price
Unclassified	Unclassified	45	A03